coatings

MDPI

*Review*

# Research Progress of Cu-Ni-Si Series Alloys for Lead Frames

**Huan Yan [1], Honglei Hu [2,*], Lei Li [3,*], Wen Huang [1] and Chunlei Li [4]**

[1] School of Materials, Shanghai Dianji University, Shanghai 201306, China; 17333636009@163.com (H.Y.); huangwen0620@163.com (W.H.)
[2] School of Mechanical Engineering, Shanghai Dianji University, Shanghai 201306, China
[3] School of Aeronautics, Shanghai Dianji University, Shanghai 201306, China
[4] School of Materials Science and Engineering, Henan Polytechnic University, Jiaozuo 454003, China; lcl2087320747@163.com
* Correspondence: huhl@sdju.edu.cn (H.H.); lilei@sdju.edu.cn (L.L.)

**Abstract:** This paper reviews the research progress of Cu-Ni-Si alloy as a lead frame material for ICs. Cu-Ni-Si alloy is considered a strong candidate for lead frame materials due to its excellent mechanical properties and adequate electrical conductivity. The types and properties of Cu-Ni-Si alloys are then discussed in detail, emphasizing strength and conductivity as two key indicators for evaluating the properties of Cu-Ni-Si alloys, as well as the challenges posed by their inverse correlation. The preparation methods of Cu-Ni-Si alloy, including conventional melting, vacuum melting, and jet forming, are also discussed, and the effects of different casting techniques on the alloy's properties are analyzed. Furthermore, the conductivity and strengthening mechanisms of Cu-Ni-Si alloy, including solid solution strengthening, second phase strengthening, and deformation strengthening, are discussed. The effects of the Ni-Si atomic ratio, trace elements, and rare earth elements on the alloy's properties are also discussed. Finally, the current research status of Cu-Ni-Si alloy is summarized, and future research directions are identified, including the development of new preparation technologies, establishment of systematic databases, and promotion of green manufacturing and sustainable alloy development.

**Keywords:** copper-nickel-silicon alloy; lead frame; strength; electrical conductivity

Academic Editor: Elena Villa

Received: 19 December 2024
Revised: 12 January 2025
Accepted: 13 January 2025
Published: 15 January 2025

**Citation:** Yan, H.; Hu, H.; Li, L.; Huang, W.; Li, C. Research Progress of Cu-Ni-Si Series Alloys for Lead Frames. *Coatings* **2025**, *15*, 91. https://doi.org/10.3390/coatings15010091

## 1. Introduction

The rapid development of electronic information technology is driving steady growth across various industries. Among them, the semiconductor industry, where integrated circuits (ICs) are the primary components, stands as a cornerstone of modern information technology. An IC consists of two primary components: the chip and the lead frame [1].

Currently, over 80% of IC lead frame materials are made from high-precision copper alloys [2]. With the development of integrated circuit technology towards large-scale integration and multifunctionality, the performance requirements for lead frame materials are becoming increasingly stringent. These include key performance indicators such as strength, heat conductivity, formability, and resistance to stress relaxation. For example, thinner strips are more conducive to etching and are designed to accommodate the high thermal dissipation requirements of integrated circuits [3]. These materials must withstand temperatures up to 500 °C, retain hardness, and ensure strong adhesion to the chip [4]. Additionally, they need to form a robust bond with brazing material to ensure the stability of wire connections [5], maintain a thickness tolerance of ± 0.005 mm to minimize stamping deformation, and exhibit good resistance to stress relaxation, among other requirements [6]. The International Annealed Copper Standard (IACS) is used to measure the electrical conductivity of materials. Specifically, conductivity is defined as the ratio of the sample's conductivity to a specific standard value, expressed as a percentage [7]. The Vickers hardness test is a method that combines the principles of both the Brinell and Rockwell hardness tests, with the Vickers hardness value denoted as HV.

The development of Cu-based lead frame materials can be divided into three stages [8,9]: the first stage features highly conductive copper alloys with electrical conductivity greater than 80% IACS and tensile strength ranging from 300 to 400 MPa, exemplified by C1220 of the Cu-P series. In the second stage, high-strength, high-conductivity copper alloys are obtained through element precipitation and strengthening processes, yielding alloys with conductivities between 60% and 79% IACS, and tensile strengths from 450 to 600 MPa. The third stage focuses on the development of high-strength, medium-conductivity copper alloys, such as Cu-Ni-Si series (e.g., KLF and C7025), designed for large-scale, lightweight integrated circuits, with tensile strengths exceeding 600 MPa and electrical conductivities around 50% IACS.

## 2. Types and Properties of Cu-Ni-Si Alloy for Lead Frame

Since the 1960s, international research has focused on copper-based lead frame materials, leveraging the excellent thermal conductivity of copper alloys, and increasing the material's strength by adding appropriate alloying elements. In the 1980s, Cu-Ni-Si alloys replaced Fe-Ni-Co alloys as the lead frame material, promoting global efforts to accelerate the development of high-strength, high-conductivity Cu-Ni-Si alloys. Strength and conductivity are the two key indicators for evaluating the properties of Cu-Ni-Si alloys, and improving these properties is essential. However, it has been found that tensile strength and conductivity of Cu-Ni-Si alloys are inversely related, meaning that an increase in tensile strength results in a decrease in conductivity, and vice versa. This inverse relationship presents a critical challenge in the research and development of Cu-Ni-Si alloys, as it complicates the optimization of material properties.

As Figure 1 illustrates, the market share of lead frames has consistently grown over the past five years. In 2023, driven by factors such as the development of new energy vehicles and the increasing intelligence of home appliances, the market share of lead frames reached USD 4.84 billion, marking a growth rate of 16.3%. With the increasing demand for lead frames, there is a growing need for higher-performance lead frames, prompting numerous companies around the world to investigate Cu-Ni-Si alloys. The main international producers of Cu-Ni-Si alloy for lead frames include Kobe Steel (Kobe, Japan), Outokumpu (Helsinki, Finland), and Olin (Clayton, MO, USA). Over 200 types of Cu-Ni-Si series alloys have been developed globally, such as C7025 (Cu-Ni-Si) from Universal Metal Products (Wickliffe, OH, USA), KLF125 (Cu-Ni-Si-Sn) alloy from Kobe Steel (Japan), and NKC114 (Cu-Ni-Si-Zn) alloy from Nikmine Metal, among others [10]. Japan, in particular, has led advancements in lead frame copper alloy technology and maintains strong international competitiveness, holding a dominant position in the global market through patent applications. The United States has likewise achieved notable advancements, realizing technological breakthroughs in lead frame copper alloys. For example, SLM Solutions introduced the $CuNi_2SiCr$ product, which meets the requirements for both strength and electrical and thermal conductivity, while also exhibiting good wear and corrosion resistance. Furthermore, this marked the first use of additive manufacturing technology for $CuNi_2SiCr$ alloys, signaling a new era in the production of Cu-Ni-Si copper-based alloys via additive manufacturing [11]. China initiated the development of lead frame copper alloys in the 1980s and has since made significant advancements, particularly in the industrial application of high-strength, high-conductivity copper alloy materials, thereby greatly enhancing product performance.

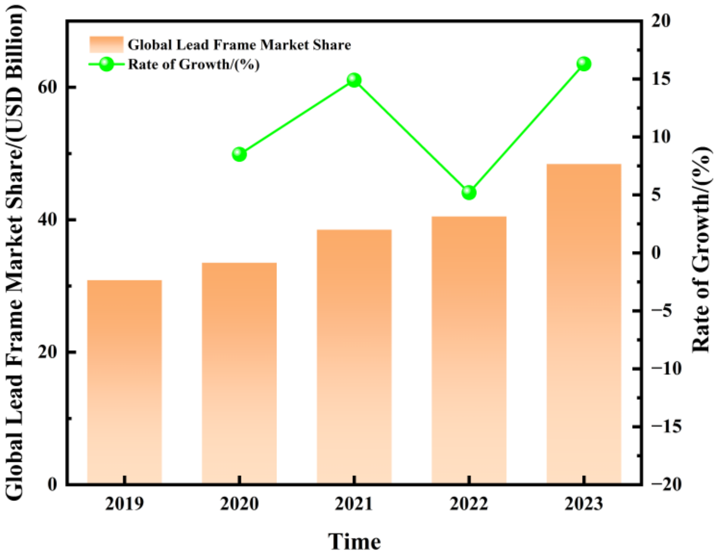

**Figure 1.** Global lead frame market share in the past 5 years.

Notably, Ningbo Xingye Shengtai Group Co., Ltd. (Ningbo, China) and Chinalco Luoyang Copper Co., Ltd. (Luoyang, China) have achieved large-scale production of C70250, C7025, QSi0.25, and QSi0.7 alloys. Additionally, Ningbo Bowei Alloy Materials Co., Ltd. (Ningbo, China) produces high-precision Cu-Ni-Si strip materials that are widely used in the market due to their high strength (yield strength up to 780 MPa), good conductivity ($\geq$40% IACS), excellent cold-working performance, outstanding fatigue resistance, and excellent bending ability. A summary of globally used Cu-Ni-Si lead frames and their performance is shown in Table 1.

**Table 1.** Commonly used Cu-Ni-Si lead frames and their performance [12].

| Alloy Grade | Alloy Composition/wt.% | Tensile Strength/MPa | Electrical Conductivity/% IACS | Elongation/% |
|---|---|---|---|---|
| C70250 | Cu-3.0Ni-0.6Si-0.1Mg | 585–690 | 35–40 | 2–6 |
| C7035 | Cu-1.5Ni-1.5Co-0.75Si | 690–970 | 45–50 | — |
| C64700 | Cu-2.0Ni-0.6Si-0.3Zn | 490–580 | 40 | 8–15 |
| C64710 | Cu-3.2Ni-0.7Si-0.3Zn | 490–580 | 40 | 8–15 |
| C7026 | Cu-2.0Ni-0.5Si | 675–780 | 40–45 | — |
| KLF-125 | Cu-3.2Ni-0.7Si-1.25Sn | 667 | 35 | 9 |
| C19010 | Cu-1.3Ni-0.25Sn-0.03P | 520–580 | 52–58 | — |
| CACTM75 | Cu-2.5Ni-0.55Si-1.0Zn-0.2Sn | 700–850 | 40–45 | — |
| C7205 | Cu-3.0Ni-0.65Si-0.15Mg | 600–800 | 35–45 | — |

## 3. Preparation of Cu-Ni-Si Alloy

Common melting techniques for Cu-Ni-Si alloys include conventional melting, vacuum melting, and jet forming. Due to the high melting points of Ni and Si, the alloy must be melted at high temperatures. Consequently, silicon is easily oxidized at these temperatures, requiring the addition of protective agents to prevent this issue. Vacuum melting allows for precise control over the content of active elements such as Al and Si, ensuring consistency in alloy composition and performance stability. However, this method can lead to crucible refractory contamination and arc melting issues, affecting the surface quality of ingot. On the other hand, the spray forming process involves atomizing the molten alloy with high-pressure inert gas and directing it into a collector, resulting in a dense, fine-grained, and homogeneous alloy.

In the production of copper alloy plates and strips, two primary casting techniques are commonly used [13]: horizontal continuous casting and down-draw semi-continuous casting, as shown in Figure 2. For Cu-Ni-Si alloys, down-draw semi-continuous casting is the more prevalent method. This process involves the formation of strip billets through down-drawing after melting, followed by hot rolling, cold rolling, heat treatment, and, ultimately, finishing and packaging. Another method is horizontal continuous casting, which begins with melting, forming strip billets through horizontal continuous casting, then cold rolling and heat treatment, and finally finishing and packaging. The production process of copper alloy sheets and strips generally follows the traditional hot rolling process which includes smelting and casting the ingot, hot rolling, cold rolling, heat treatment, finishing, and packaging for storage.

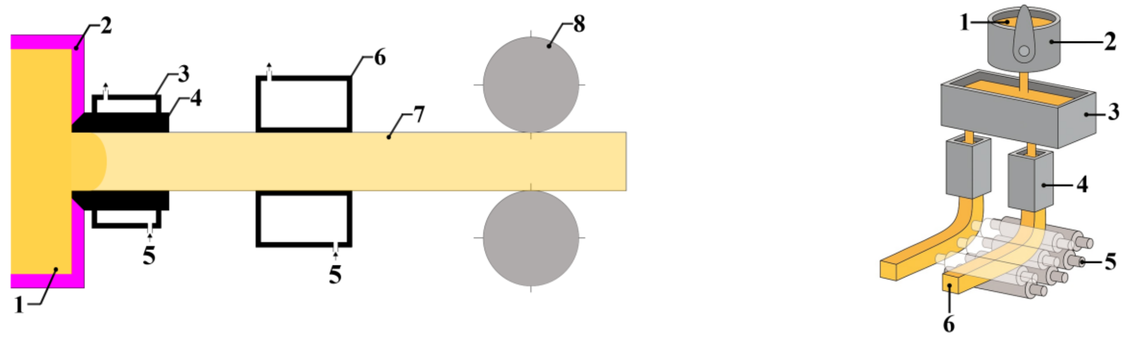

**1. Melt 2. Heat holding furnace 3. Cold water crystallizer 4. Graphite sleeve 5. Condensate 6. Secondary cooling 7. Ingot 8. Drawing roll**

**1.Melt 2.Ladle 3.Tundish 4.Mold+Cooling system 5.Rollers 6.Copper strand**

**Figure 2.** Two casting methods for copper alloys: (**a**) horizontal continuous casting and (**b**) down-draw semi-continuous casting.

To meet the demands for miniaturization and high integration in electronic devices, the thickness of the frame material has been reduced to 0.015 mm [14]. Typically, its width and spacing are 80% of the plate thickness. Thinner strips are more conducive to etching processes, but the thickness varies depending on the working environment, generally ranging from 0.015 mm to 0.6 mm.

W. Liao [15] prepared strip Cu-2.79Ni-0.58Si-0.1Mg alloy (C70250 copper alloy) using both cold mold continuous casting (CMCC) and hot mold continuous casting (HMCC) methods, and investigated the effects of deformation rate on the alloy. The results indicate that the strips produced by the CMCC process were characterized by equiaxial particles, while those from the HMCC process exhibited columnar particles. When the deformation amount reaches 98%, cracks and spalling occur on the surface of the equiaxial grain zone, while the columnar grain zone showed no such defects and maintained superior surface quality, as shown in Figure 3. At this point, the elongation of the columnar grain strip remains as high as 3.2%, which is 2.9 times higher than that of the equiaxed grain alloy. The residual stress in the equiaxed grain zone reaches 363 MPa, which is 2.7 times higher than that in the columnar grain zone. Following cold rolling with significant deformation, the elongation and ductility of the columnar grain strip are enhanced, and the residual stress is substantially reduced. Consequently, the HMCC process is more appropriate for large deformation cold rolling of C70250 copper alloy.

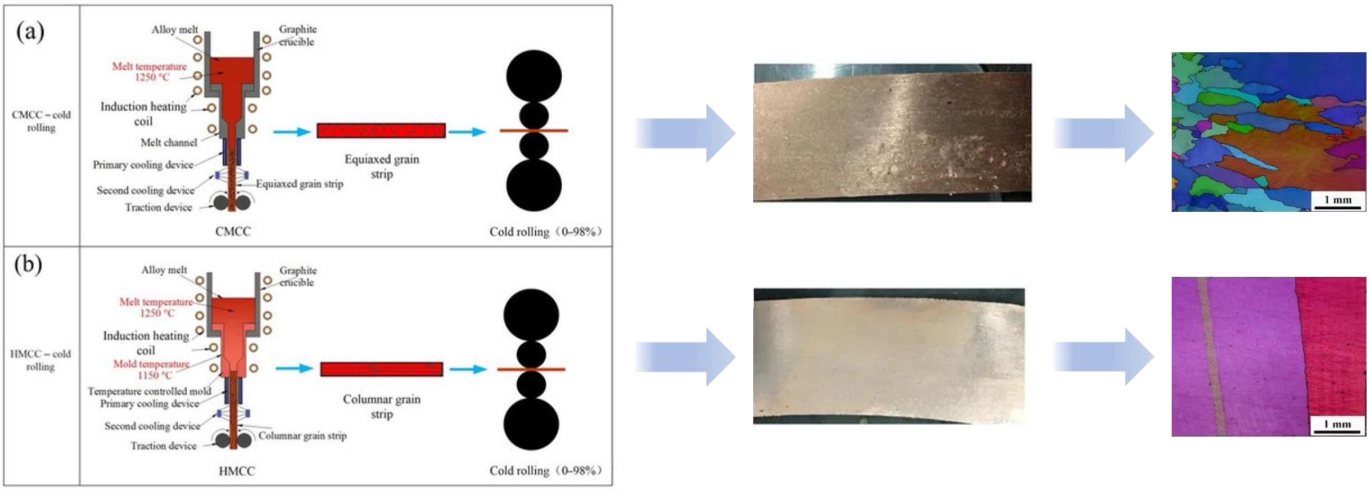

**Figure 3.** Schematic diagram of the preparation and cold rolling process of C70250 copper alloy strip and the surface morphology and microscopic morphology of the strip under 98% cold deformation [15]: (**a**) CMCC and (**b**) HMCC.

Another method for preparing copper alloys is the spray deposition process, which involves introducing molten metal into an atomizing chamber and spraying it through a nozzle at high speed under the protection of high-pressure inert gas to create atomized and dispersed fine droplets. These droplets are propelled towards the depositor by the high-speed gas flow, and various shapes and motion modes of the depositor are employed [16]. Consequently, blank parts of various shapes and specifications can be produced. The alloy blanks manufactured by spray deposition exhibits superior densification, reduced segregation, and a uniform structure [17]. The spray deposition process is depicted in Figure 4. Currently, this process is extensively utilized for the production of lead, magnesium alloys, and steel, yet it encounters challenges when applied to copper alloy materials. Ashish Agrawal [18] fabricated Cu-Al-Ni shape memory alloy strips using a spray deposition and hot rolling process. The results indicate that, compared to the traditional casting process, the fabricated Cu-Al-Ni SMA strips exhibit finer grain sizes, superior strength, and enhanced ductility. However, the complexity of the preparation process significantly hinders its broad application in the production of Cu-Ni-Si alloys. It is essential to develop tailored spray deposition and rolling processes for Cu-Ni-Si alloys to fabricate ultra-thin, high-performance Cu-Ni-Si alloys.

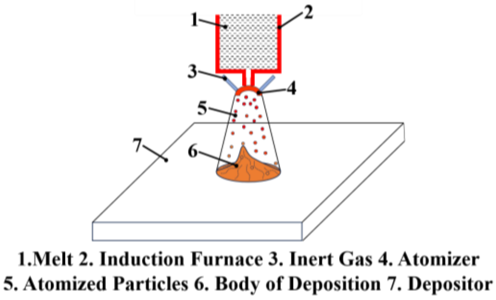

**Figure 4.** Spray deposition diagram.

## 4. Conductivity and Strengthening Mechanism of Cu-Ni-Si Alloy

### *4.1. Conduction Mechanism of Cu-Ni-Si Alloy*

The main factors affecting the resistivity of Cu-Ni-Si alloy include solid solubility of solute atoms, the volume fraction of the precipitated phase, the degree of coherence between the precipitated phase and matrix, and the structural defects caused by work hardening. Among these factors, the degree of solid solubility of solute atoms has the greatest influence on the resistivity of Cu-Ni-Si alloy [19].

Cu-Ni-Si alloys are classified as age-hardenable, precipitation-strengthened alloys. According to the Mathiessen rule, the resistivity of Cu-Ni-Si alloy is given by [20]:

$$\rho_S = \rho_O + \Delta\rho_{GB} + \Delta\rho_p + \Delta\rho_S + \Delta\rho_d \tag{1}$$

In the formula, $\rho_O$ represents the resistivity of the solvent phase in the solid solution. $\Delta\rho_{GB}$ represents the resistivity change caused by grain boundary strengthening. $\Delta\rho_p$ is the resistivity change caused by solid solution atoms. $\Delta\rho_S$ represents the resistivity change caused by solute atoms in solid solution. $\Delta\rho_d$ represents the resistivity change caused by work hardening.

When a solute atom enters the copper matrix, lattice distortion occurs due to differences in atomic size. This distortion causes increased scattering of electron motion, which in turn reduces the conductivity of the alloy. The influence of solute atoms on the conductivity of the alloy is different. As shown in Figure 5, Co, Si, P, Fe, and other elements have a significant effect on the conductivity of the alloy. In the design of alloy composition, the amount of these elements should be controlled. To minimize the effect of solute atoms on the lattice distortion, it is preferable to select solute atoms that exhibit significant temperature-dependent solubility, with low solubility at low temperatures, and low residual resistance. Aging treatment can relieve the strain energy accumulated during the process, promote the second phase precipitation from the supersaturated solid solution, purify the matrix, and improve the electrical conductivity.

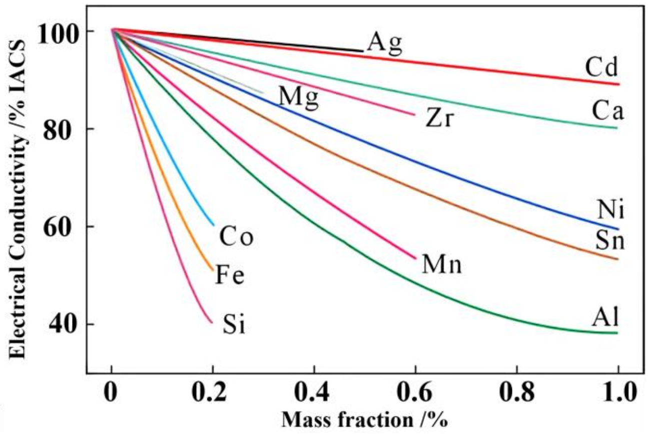

**Figure 5.** Effect of alloying elements on the electrical conductivity of copper alloys [11].

### 4.2. Strengthening Mechanism of Cu-Ni-Si Alloy

Typically, the investigation of high strength and conductivity Cu alloys frequently involves a trade-off between strength and conductivity. Generally, the incorporation of alloying elements diminishes the electrical conductivity of Cu alloys. Furthermore, the strength improvement from solid solution strengthening is often limited. Consequently, it is crucial to explore alternative strengthening mechanisms that can substantially enhance the strength of Cu alloys without compromising their EC. High-strength and high-conductivity Cu alloys are primarily strengthened through second-phase strengthening (precipitation strengthening), solid solution strengthening, deformation strengthening (dislocation strengthening), and other strengthening mechanisms.

For precipitation-strengthened Cu alloys, the total yield strength can be determined using the following formula [21]:

$$\sigma_{total} = \sigma_0 + \Delta\sigma_p + \Delta\sigma_{SS} + \Delta\sigma_{GB} + \Delta\sigma_d \tag{2}$$

where $\sigma_0$ denotes the intrinsic lattice stress; $\Delta\sigma_p$ represents precipitation strengthening; $\Delta\sigma_{SS}$ signifies solid solution strengthening; $\Delta\sigma_{GB}$ indicates fine grain strengthening; and $\Delta\sigma_d$ corresponds to dislocation strengthening.

### 4.2.1. Second-Phase Reinforcement

The yield strength of precipitated Cu alloys is closely associated with the structure, size, morphology, and distribution of the precipitated phase. By optimizing the composition, selecting the appropriate strengthening phase, employing the suitable process route, controlling the structure, size, volume fraction, and distribution of the precipitated phase, as well as the orientation relationship between the precipitated phase and the Cu matrix, Cu alloys can achieve excellent comprehensive properties while maintaining high electrical conductivity. For Cu alloys strengthened by precipitation under peak aging and over-aging conditions, the Orowan mechanism is the predominant strengthening mechanism, and the Orowan stress ($\Delta\sigma_p$) can generally be expressed as [22]:

$$\Delta\sigma_p = 0.81 \times \frac{MGb}{2\pi(1-v)^{1/2}} \times \frac{\ln\left(\frac{d}{b}\right)}{\lambda} \tag{3}$$

In the formula, $M$ represents the Taylor factor (3.1), $G$ denotes the shear modulus (48 GPa), $b$ is the Berger vector (0.2556), $v$ is the Poisson's ratio (0.34), $d$ is the particle diameter intersecting the slip plane, and $\lambda$ is the effective particle spacing accounting for the obstacle size effect.

The main strengthening phase of Cu-Ni-Si alloy is δ-$Ni_2Si$ intermetallic compound [23–28]. In addition, Teplitskiy et al. [29] reported that the δ-$Ni_2Si$ precipitates in Cu-Ni-Si alloys with low Ni and Si contents are disc-shaped. For triangular arrays with an ideal uniform distribution of disc-shaped δ-$Ni_2Si$ particles of thickness $t$ and diameter $d_p$, the relationship between the volume fraction ($F_v$) and the average center-to-center distance between particles ($\lambda_s$) can be expressed as follows:

$$F_v = \frac{\sqrt{3}\pi d_p^2 t}{8\lambda_s^3} \tag{4}$$

If the disc-plane of $Ni_2Si$ particles is parallel to the slip plane (as depicted in Figure 6a,b), ($\lambda = \lambda_s - d_p$) the effective inter-particle spacing is given by the formula:

$$\lambda = \left(\frac{\sqrt{3}\pi d_p^2 t}{8F_v}\right)^{1/3} - d_p \tag{5}$$

Substituting Equation (5) into Equation (3), the yield strength increment for the Cu alloy reinforced with disk-like $Ni_2Si$ particles is given as:

$$\Delta\sigma_p = 6035.3 \times \frac{\ln(d/0.2556)}{\left(\frac{\sqrt{3}\pi d_p^2 t}{8F_v}\right)^{1/3} - d_p} \tag{6}$$

If the disc-plane of $Ni_2Si$ particles is perpendicular to the slip plane (as depicted in Figure 6c,d), the effective inter-particle spacing is expressed as:

$$\lambda = \left(\frac{\sqrt{3}\pi d_p^2 t}{8F_v}\right)^{1/3} - \frac{1}{2}d_p - \frac{\sqrt{3}}{2}t \tag{7}$$

The yield strength increment can also be expressed as:

$$\Delta\sigma_p = 6035.3 \times \frac{\ln(d/0.2556)}{\left(\frac{\sqrt{3}\pi d_p^2 t}{8F_v}\right)^{1/3} - \frac{1}{2}d_p - \frac{\sqrt{3}}{2}t} \tag{8}$$

Assuming spherical particles are distributed on a square lattice, a valid simplification for a small volume fraction of precipitates, the yield strength increment can be expressed using the following Orowan–Ashby equation:

$$\Delta\sigma_p = 0.81 \times \frac{MGb}{2\pi(1-v)^{1/2}} \times \frac{\ln(d_p/b)}{\frac{1}{2}d_p\sqrt{\frac{3\pi}{2F_v}} - d_p} \tag{9}$$

Lei et al. [30] computed the relationship between the average size of precipitates and Orowan strengthening ($F_v$ = 0.14%), as depicted in Figure 7. It has been observed that the average particle size significantly influences the increase in $\Delta\sigma_{\text{orowan}}$ when the average particle size is less than 50 nm. Yi et al. [31] reported that the thickness of disk-like δ-$Ni_2Si$ precipitates is approximately 2 nm, and the growth along the radial direction exceeds that along the thickness direction. According to the above formula, both the decrease of mean diameter ($d_p$) and the increase of volume fraction ($F_v$) can lead to the increase of yield strength increment.

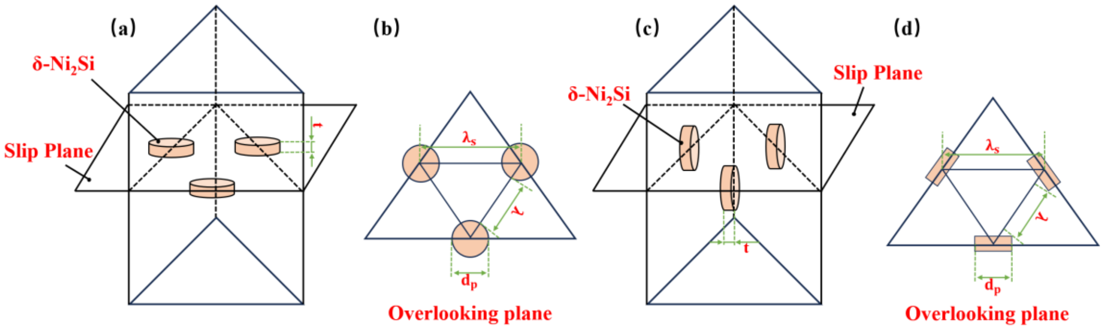

**Figure 6.** Arrangement of disc-shaped $Ni_2Si$ particles within a triangular prismatic volume of the Cu matrix: (**a**,**b**) disc-plane parallel to the slip plane, and (**c**,**d**) disc-plane perpendicular to the slip plane.

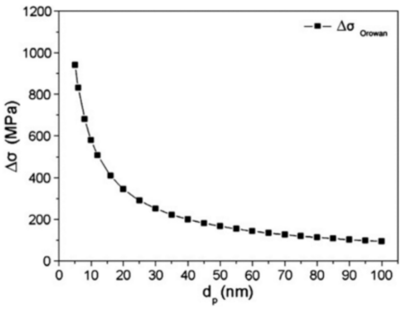

**Figure 7.** Schematic representation of Orowan strengthening attributed to the average size of precipitate particles.

The KLFA85 alloy, developed by Kobe Steel in Japan, forms $Ni_2Si$ phase particles following aging treatment, resulting in a tensile strength of 800 MPa and an electrical conductivity of 45% IACS. The EFTEC-64T alloy, developed by Furukawa Electric Industry Company (Tokyo, Japan), possesses a conductivity of 80% IACS and a tensile strength of 539 MPa [32,33]. M. Goto's study [34] found that in Cu-6Ni-1.5Si alloy, a nanoscale disc-shaped continuous precipitate (CP), δ-$Ni_2Si$, forms during normal aging. Over-aging resulted in the development of fibrous, discontinuous precipitates (DPs), which were stable δ-$Ni_2Si$ fibrous precipitates distributed in the copper matrix. The DP phase exhibits superior conductivity and tensile strength compared to the CP phase. Additionally, cold deformation prior to aging facilitates the precipitation of fine dispersion phases, increasing the alloy's strength with minimal reduction of conductivity. These studies demonstrate that second-phase strengthening can also enhance the conductivity of Cu-Ni-Si alloys. However, the impact of precipitated phase characteristics, such as structure, size, morphology, and distribution, particularly for δ-$Ni_2Si$, on the conductivity of Cu-Ni-Si alloys remains unexplored. Consequently, achieving effective control over precipitate growth and maximizing their contribution to strength is anticipated to be a significant breakthrough in future research.

#### 4.2.2. Deformation Strengthening

Deformation strengthening refers to the phenomenon where the material's strength and hardness increase with increasing deformation after yielding, while the plasticity and toughness correspondingly decrease [35]. This strengthening mechanism is due to the increase in dislocation density during plastic deformation. Concurrently, the dislocation pinning effect is enhanced, and grain breakage occurs, leading to the formation of vacancies and residual stress, which promote the formation of second-phase particles [36]. Consequently, the strength of Cu alloys increases with an increase in dislocation density, and the yield strength increment due to dislocation strengthening can be calculated using the Taylor equation [37]:

$$\Delta\sigma_p = M\alpha Gb\rho^{1/2} \tag{10}$$

In the formula, $M$, $G$, and $b$ retain the meanings described previously; α is a constant; and $\varrho$ represents the dislocation density, which can be derived from X-ray diffraction analysis.

As per Equation (10), the dislocation number density directly determines the contribution of dislocation strengthening. By employing appropriate treatment and adjusting the dislocation density, the dislocation strengthening of Cu alloys can achieve higher strength. Furthermore, the crystal defects generated during plastic deformation have minimal impact on electrical conductivity and can be restored in subsequent processes. Consequently, the high electrical conductivity of Cu alloys can be maintained through dislocation strengthening. However, the ability to enhance the alloy's strength solely through deformation strengthening is limited. Therefore, it is often necessary to integrate deformation strengthening with other strengthening mechanisms.

H. Wei et al. [38] studied the effect of various degrees of cold rolling deformation on the properties of Cu-3.0Ni-0.60Si-0.16Zn-0.15Cr-0.03P alloy and determined the optimal cold rolling deformation and aging process parameters. By fine-tuning these parameters, they observed that the alloy, subjected to 95% cold rolling and aged at 450 °C for 60 min, exhibited a significant improvement in ultimate tensile strength of 841 ± 10 MPa and electrical conductivity of 52.2 ± 0.3% IACS. The Cu-Ni-Si alloy exhibits excellent properties, with a strength of 607 MPa and an electrical conductivity of 53% IACS, after undergoing 760 °C for 0.5 h solution treatment, followed by 40% cold deformation and 480 °C for 2 h aging treatment [39].

In the actual production process, cold deformation is an effective method for strengthening metals, which can improve the material's strength, but may also increase the risk of brittle fracture, increase energy consumption, and reduce electrical and thermal conductivity. Therefore, the degree of cold deformation must be carefully controlled during processing, and combined with appropriate heat treatment to ensure optimum performance. As a precipitation-strengthened alloy, Cu-Ni-Si alloy benefits from the synergistic action of various strengthening mechanisms. It is important to note that thermal stability could be a significant concern, necessitating the implementation of suitable heat treatment or alloying strategies in practical applications.

### 4.2.3. Solid Solution Strengthening

Solution strengthening refers to the method of adding alloying elements to a matrix to form a solid solution, which interacts with dislocations to enhance the alloy's strength [40]. The strengthening effect primarily relies on the atomic size difference between the solute and the matrix, as well as the solute's concentration in the matrix. The incorporation of solute atoms significantly reduces the alloy's electrical conductivity. Cu alloys are typically strengthened through a combination of solid solution strengthening and aging strengthening. The increase in yield strength due to solid solution strengthening can be calculated as [41]:

$$\Delta\sigma_{SS} = M\frac{G\varepsilon_{SS}^{3/2}c^{1/2}}{700} \tag{11}$$

$$\varepsilon_{SS} = \left|\frac{\varepsilon_G}{1+\frac{1}{2}|\varepsilon_G|} - \beta\varepsilon_b\right| \tag{12}$$

$$\varepsilon_G = \frac{1}{G}\frac{dG}{dc} \tag{13}$$

$$\Delta\varepsilon_b = \frac{1}{a}\frac{da}{dc} \tag{14}$$

In the formula, $\varepsilon_{SS}$ represents the mismatch strain induced by lattice distortion from neighboring solute atoms, $\beta$ is a constant, $a$ denotes the lattice parameter of the Cu matrix, $\varepsilon_b$ and $\varepsilon_G$ are the correction coefficients for solid solution atomic lattice parameters and shear modulus, respectively, and $c$ signifies the atomic concentration of residual solid solution atoms in the matrix. For precipitation-strengthened Cu alloys, the contribution of solid solution strengthening to yield strength is minimal.

Furthermore, in typical low-concentration solid solutions, the variation of yield stress with solute concentration can be represented as [42]:

$$\sigma = \sigma_0 + KC^m \tag{15}$$

In the formula, $\sigma$ represents the yield stress of the alloy; $\sigma_0$ denotes the yield stress of the pure metal; $C$ signifies the atomic concentration of the solute; $K$ and $m$ are constants associated with the alloy elements and properties, and the value of m ranges from 0.5 to 1.

Ren Wei et al. [43] emphasized that the strength of precipitation-strengthened copper alloys depends on three key factors: the concentration of solute elements in the matrix, the volume fraction of the precipitated phase, and grain size. In the case of Cu-Ni-Si alloy, a typical precipitation-strengthened alloy, the increase in strength due to solid solution strengthening is less pronounced when the solution treatment temperature is below 850 °C. This is due to the low solubility of solute elements in the matrix at low solution treatment temperatures, which results in a limited solution strengthening effect. However, aging treatment can promote the formation of the precipitated phase, significantly improving the alloy's strength. This process, which involves the change in solid solubility of alloying elements at high temperatures and the subsequent diffusion of elements, plays a crucial role in the strengthening mechanism of

Cu-Ni-Si alloys. Therefore, solution strengthening is often combined with other strengthening methods, such as deformation strengthening and aging strengthening.

As a precipitation-hardened alloy, Cu-Ni-Si relies on the synergistic action of various strengthening mechanisms to achieve optimal strength. For instance, cold deformation is commonly applied before aging treatment to refine and disperse the secondary phase, thereby facilitating precipitation and achieving alloy strengthening. By adopting this integrated strengthening approach, the alloy's properties are optimized, improving its reliability and performance in various applications.

## 5. Cu-Ni-Si Alloy Composition Design

### *5.1. Influence of Ni-Si Atomic Ratio on Cu-Ni-Si Alloy*

Lockyer [44] first reported the significant influence of the Ni to Si content ratio on the properties of Cu-Ni-Si alloys in 1994. As the Cu-Ni-Si alloy exhibits an obvious aging strengthening effect, a significant amount of $Ni_2Si$ phase is precipitated during aging. The mass ratio of Ni to Si not only determines the microstructure of the alloy, but also significantly affects its physical and chemical properties. The research of J. Li et al. [45] indicates that the hardness and conductivity of Cu-Ni-Si alloys are influenced by the Ni/Si mass ratio. Optimal hardness occurs when the Ni/Si ratio is 3.6–5.1, with a maximum hardness of 238 HV at 4.2. Maximum conductivity is achieved when the Ni/Si ratio is 4.2–6.2, peaking at 43.7% IACS at 5.1. Overall, the properties of the alloy are best when the Ni/Si mass ratio is between 4 and 5.

The precipitation behavior of the alloy directly affects its comprehensive properties. In addition, the precipitation order, size, morphology, microstructure, and distribution of the precipitated phase are all affected by aging conditions and alloy composition. Hu et al. [25] studied the precipitation sequence and evolution process of δ-$Ni_2Si$ phase in Cu-2.4Ni-0.7Si-0.4Cr (wt.%), as shown in Figure 8.

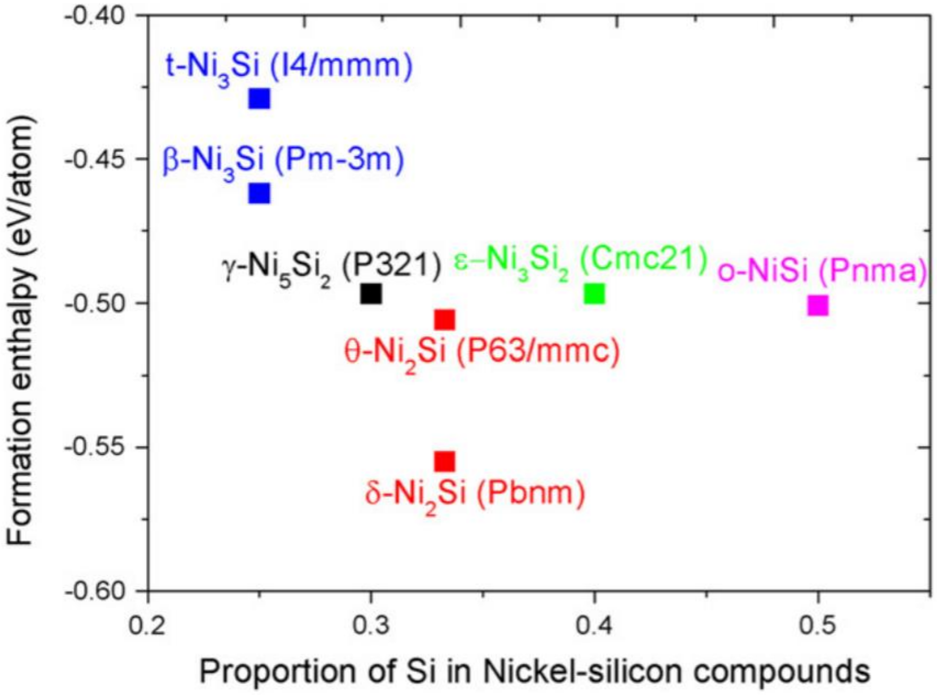

**Figure 8.** The formation enthalpies of various nickel-silicon compounds as a function of Si content [25].

S. Tao et al. [46] demonstrate that as the Ni/Si mass ratio increases, the alloy's conductivity and hardness initially rise and then decline. When the Ni/Si mass ratio reaches 4:1, an optimal balance between these properties is achieved. The impact of the Ni/Si ratio on the conductivity of Cu-Ni-Si alloys is primarily due to the residual amounts of Ni and Si in the Cu matrix following aging treatment. Cu-Ni-Si alloys subjected to solution and aging, as depicted in Figure 9(a,a1,b,b1), exhibit limited solubility in Cu when the Si content is high, leading them to exist as elemental powder, and thereby increasing defects. Si diffuses towards the grain boundary, and due to its faster diffusion rate, a small amount of δ-$Ni_2Si$ particles precipitate and distribute along the grain boundary. No granular or acicular precipitates were detected in the Cu matrix. As illustrated in Figure 9c, when the Ni/Si ratio is 4:1, the number of δ-$Ni_2Si$ particles at the boundary is significantly reduced, and numerous flocculent particles are present. Figure 9(c1) depicts the presence of a fibrous phase in the Cu matrix. As depicted in Figure 9(d1), when the Ni/Si ratio is 5:1, there are only a few flocculent particles. Concurrently, compared to Figure 9c, the δ-$Ni_2Si$ phase precipitated in Figure 9d is also reduced. When the Ni/Si ratio approaches the stoichiometric ratio of the δ-$Ni_2Si$ phase, the majority of Ni and Si atoms precipitate into this phase, thereby achieving the highest electrical conductivity. The authors hypothesize that these fibrous phases are δ-$Ni_2Si$ based on X-ray diffraction (XRD) results; however, δ-$Ni_2Si$ typically exhibits a disc-like shape [47], which can vary depending on the processing conditions. For further confirmation, energy-dispersive spectroscopy (EDS) can be employed to ascertain the chemical composition of these white flocculent particles. If they primarily consist of Ni and Si, they are likely the δ-$Ni_2Si$ phase; however, if they also contain other elements, such as copper or oxygen, they may represent a different phase.

The atomic ratio of Ni/Si has a significant effect on the hardness and conductivity of Cu-Ni-Si alloys, as shown in Table 2. Despite extensive studies on the impact of the Ni/Si atomic ratio on the mechanical and electrical properties of Cu-Ni-Si alloys, no consensus has been reached. Researchers continue to explore ways to adjust the Ni/Si ratio in order to optimize the alloy's strength and conductivity.

**Table 2.** The relationship between Ni and Si content and hardness and conductivity of the alloy [48].

| Alloy Composition/wt.% | Dimensional Hardness/HV | Electrical Conductivity/% IACS |
|---|---|---|
| Cu-1.0Ni-0.23Si | 122 | 61.0 |
| Cu-1.5Ni-0.34Si | 173 | 56.3 |
| Cu-2.0Ni-0.47Si | 190 | 18.4 |
| Cu-2.5Ni-0.58Si | 215 | 41.7 |
| Cu-3.0Ni-0.72Si | 232 | 39.9 |

The chemical composition of the alloy affects the performance and service conditions of the product, and also affects its subsequent processing technology and material processing performance. To fully harness the material's potential across various service environments, it is crucial to carefully match the matrix metal with the alloying components in order to achieve the best overall performance. This approach, which considers chemical composition, processing techniques, and service conditions, is key to achieving high-performance alloy design.

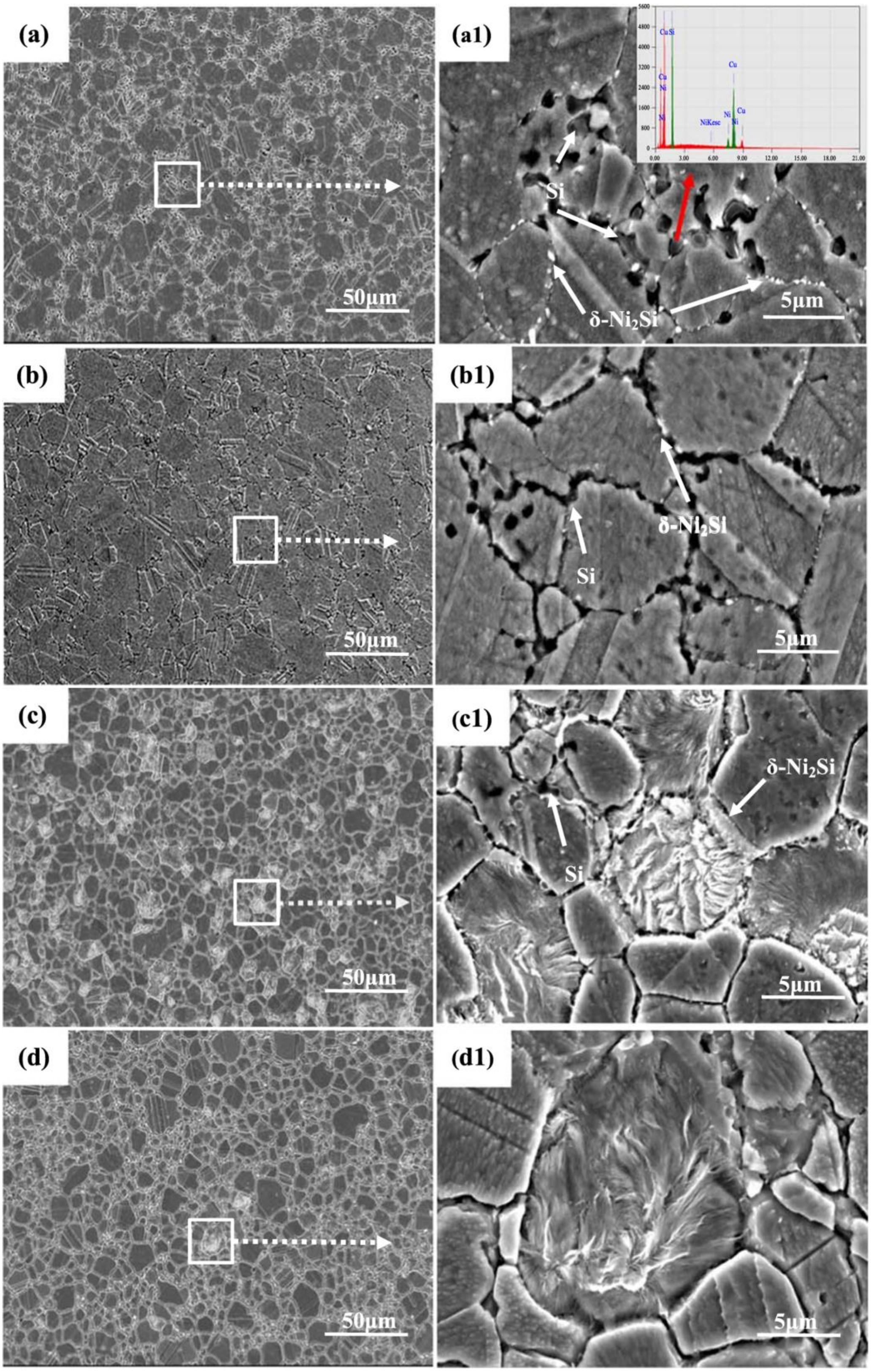

**Figure 9.** SEM microstructures of as-sintered Cu-Ni-Si alloys after solid solution treatment, where the mass ratios of Ni to Si are (**a**) 2:1, (**b**) 3:1, (**c**) 4:1, and (**d**) 5:1, (**a1**–**d1**) are the local enlarged images of (**a**–**d**), respectively [46].

### 5.2. Influence of Trace Elements on Alloys

With the rapid development of industrialization and information technology, the demand for Cu-Ni-Si alloys continues to grow. Traditional alloy composition adjustment and processing methods are no longer sufficient to meet the increasingly stringent performance requirements. As a result, researchers are exploring ways to improve the overall properties of alloys by incorporating specific ratios of various alloying elements, as shown in Table 3. The addition of manganese (Mn) can improve both the strength and ductility of the alloy [49], and cobalt (Co) can effectively prevent the migration of vacancies and also promote the precipitation of the second phase during the aging hardening process. Zinc (Zn) can enhance the adhesion between copper alloys and solder. For different applications, it is important to select the appropriate elements and precisely control their concentrations.

**Table 3.** Influence of trace element type and content on hardness and conductivity of alloy.

| Alloy Composition/wt.% | Dimensional Hardness/HV | Electrical Conductivity/% IACS |
|---|---|---|
| Cu-3Ni-0.5Si-3Ti [50] | 268 | 33.8 |
| Cu-1.5Ni-0.6Si-1.0Co [51] | 250 | 43.0 |
| Cu-2Ni-1Si-0.8Ag [52] | 193 | 29.3 |
| Cu-3.2Ni-0.7Si-0.3Zn [53] | 250 | 60.0 |
| Cu-4.74Ni-1.19Si-0.096Cr [54] | 250–270 | 46–47 |
| Cu-2Ni-0.5Si-0.15Zr [55] | 163.8 | 47.5 |
| Cu-6Ni–1Si-0.5Al-0.15Mg-0.1Cr [56] | 343 | 28.1 |
| Cu-2.89Ni-0.61Si-0.14Mg-0.2Nb [57] | 245.9 | 4.7 |
| Cu-0.9Ni-0.1Si-1.9Sn-0.1P [58] | 224.2 | 36.4 |
| Cu-3.57Ni-1.8Ti-0.85Si-1Diamond [59] | 291.1 | 40 |

The addition of appropriate amounts of additional elements can significantly improve both the tensile strength and conductivity of Cu-Ni-Si alloy, with the effects of these elements varying depending on their type and content. By precisely controlling the type and content of trace elements, the alloy can be tailored to meet the specific requirements of different applications. This versatility enables Cu-Ni-Si alloys to be optimized for a wide range of engineering and industrial uses, ensuring that their performance is well-suited to the demands of diverse operating conditions.

### 5.3. Influence of Rare Earth Elements on Alloys

Rare earth elements exhibit reactivity with a variety of elements due to their active chemical properties. China, with its abundant rare earth resources, began exploring their application in copper alloys as early as the 1960s. The primary effects of rare earth elements on copper alloys are as follows [60,61]: (1) refining the grain structure, optimizing the morphology and distribution of impurities, and enhancing corrosion and wear resistance; (2) purifying the alloy structure through deoxidation and desulfurization, thereby enhances casting performance; and (3) forming stable compounds with hydrogen to prevent hydrogen embrittlement and optimize the metallographic structure.

J.-S. Liu and colleagues [62] studied the effects of the micro-addition of lanthanum (La) content on the as-cast macrostructure, physical properties, and corrosion resistance of Cu-Ni-Si alloy (C7025). It was found that the as-cast structure was significantly refined when an optimal amount of lanthanum (La) was added. As the lanthanum (La) content increased, the second phase transitioned from granular to elongated and dispersed along the grain boundary. Both the yield strength and tensile strength of the Cu-Ni-Si alloys followed an “M”-shaped trend as lanthanum (La) content increased. Additionally, the corrosion resistance of the alloy was improved with the optimal lanthanum (La) addition, with a mass fraction of 0.17% showing the best performance. X.-J. Li and colleagues [63] studied the effect of rare earth cerium (Ce) addition on the microstructure and properties of Cu-3.0Ni-0.64Si alloy. The experimental results show that the optimal addition of cerium (Ce) can purify the material by removing impurities, refining grains, and improving both the tensile strength and electrical conductivity. T.-Y. Wang and colleagues [64] studied the effect of erbium (Er) on Cu-Ni-Si alloy. They found that adding 0.1% erbium (Er) significantly improved the strength and hardness of the alloy without compromising its plasticity or conductivity. However, excessive erbium (Er) reduced the alloy's plasticity.

Despite these advancements, the utilization of rare earth elements in copper alloys is still in its infancy, particularly with respect to ingot production technology. Due to the high oxygen affinity of rare earth elements, they are prone to oxidation, which is why vacuum melting technology is frequently employed to mitigate oxidation losses. To improve the quality of ingots in non-vacuum melting processes, further optimization of melting process parameters is necessary to ensure ingots with high density and uniform microstructure. Furthermore, the exact mechanism by which rare earth elements influence the microstructure and properties of alloys remains incompletely understood, presenting significant opportunities for further research in this domain.

## 6. Processing Technology of Cu-Ni-Si Alloy

### *6.1. Influence of Solution Technology on Alloy Properties*

The main goal of solid solution treatment is to dissolve impurities and precipitates in the matrix to form a saturated solid solution, thereby promoting the precipitation of a fine and uniformly distributed strengthening phase during subsequent aging, which enhances the alloy's strength. In addition, it helps to eliminate the stresses induced by hot and cold processing, promotes recrystallization, and prepares for the subsequent aging treatment.

H.-S. Wang et al. [65] studied a Cu-7.4Ni-1.3Si-1.2Cr alloy prepared by powder metallurgy, and examined the effects of various solution-aging heat treatment parameters on microstructure evolution and its impact on mechanical and thermal properties. Research indicates that the thermal conductivity of powder metallurgy copper alloys decreases after a specific solution heat treatment, and the subsequent aging treatment can improve the thermal conductivity. The optimal heat treatment process involves solution treatment at 970 °C for 8 h followed by aging at 450 °C for 1 h. This regimen ensures that the subgrain size of the powder metallurgy copper alloy is less than 30 μm, and the tensile strength of the alloy is 820 MPa.

Although solution treatment can enhance the strength of the alloy, it may also reduce the conductivity. In practical applications, the solid solution treatment is often incomplete, leading to the precipitation of solute atoms during hot rolling. This precipitation diminishes the strengthening effect of second-phase particles during subsequent aging, resulting in a tensile strength lower than the anticipated value.

### *6.2. Influence of Hot Deformation Process on Alloy Properties*

Through thermal deformation, a recrystallized structure with good mechanical properties can be obtained. The mechanisms of metal thermal deformation include slip deformation, twin deformation, grain boundary sliding, and diffusion creep [66]. The main factors affecting these deformation mechanisms are the microstructure and deformation temperature of the metal materials. These factors collectively determine the deformation behavior and final microstructure of metal materials, which in turn determine the macroscopic mechanical properties.

The research of G. Cao [67] indicates that the key factor affecting the degree of dendrite segregation and recrystallization is the alloy composition. After hot rolling, a clear grain orientation develops, and recrystallization occurs to a certain extent. At the same time, this process also results in increased lattice distortion, which significantly reduces electrical conductivity. The research of Y. Wang [68] demonstrates that the mechanical properties of an Al-Mg-Si-Cu alloy after hot rolling are influenced not only by the microstructure, but also by the texture developed during the rolling process. With the increase of hot rolling reduction, dislocation stacking becomes more significant, and stacking defects accumulate near the subgrain boundaries. The formation of shear texture contributes to an increase in both ultimate tensile strength and yield strength. These findings highlight the importance of alloy composition in controlling the microstructure and properties, as well as the influence of microstructure evolution on the final properties during hot rolling.

In industrial practice, the advantages of thermal deformation are readily apparent. Compared to traditional reduction processes, hot deformation produces no metal waste during processing. It alters the shape and enhances the plasticity and toughness of the metal, and has high productivity, making it suitable for industrial mass production. These characteristics render thermal deformation an important technology for enhancing material utilization and production efficiency.

### *6.3. Influence of the Aging Process on Alloy Properties*

Cu-Ni-Si alloy, which is precipitation-strengthened, primarily gains strength through the precipitation of fine $Ni_2Si$ phases during the aging process [69]. These precipitates are typically only a few nanometers in size. However, prolonged aging times can cause them to coarsen to tens of nanometers, thereby diminishing the strengthening effect. Consequently, it is crucial to accurately control the aging time to maintain the optimal strengthening effect and preserve the desired properties of the alloy.

The aging treatment is crucial for enhancing the strength of Cu-Ni-Si alloys, garnering considerable scholarly attention worldwide. Y.-H. Li et al. [70] pointed out that $\delta$-$Ni_2Si$ precipitate is the key strengthening phase in Cu-Ni-Si alloys, and its coarsening behavior significantly impacts the mechanical properties of the materials. Through systematic investigation, the coarsening process of $\delta$-$Ni_2Si$ precipitates during over-aging treatment is systematically investigated. It has been observed that the core structure of $\delta$-$Ni_2Si$ remains stable, while its outer shell consists of Cu, Ni, and Si elements, forming metastable interfaces. In the later stages of over-aging, this core–shell structure will completely transform into a stable $\delta$-$Ni_2Si$ phase associated with the Cu matrix. S.J. Lee [71] et al.'s research showed that Cu-6wt.%Ni-1.4wt.%Si alloy was prepared by water quenching (solution treatment) or air cooling (homogenization treatment) after heating at 980 °C for 2 h and aging at 500 °C for 6 h. After maintaining the high-temperature single-phase, the microstructure of the precipitated phase in the matrix changes significantly with the cooling rate. In the solution-treated alloy, the precipitates appear as discontinuous fibrous structures, whereas the homogenized alloy exhibits well-defined spherical particles. The strength, ductility, and conductivity of the homogenized alloy are 628 MPa, 18%, and 48% IACS, respectively, which are higher than those of the solution-aged alloy, with 582 MPa, 15.5%, and 50% IACS, respectively. These findings are crucial for understanding and controlling the aging treatment of Cu-Ni-Si alloys.

F. Qi [72] et al. enhanced the comprehensive properties of the Cu-Ni-Si alloy via multi-pass continuous extrusion and aging treatment, as depicted in Figure 10. In the figure, 1P, 2P, 3P, and 4P denote the number of repeated extrusion cycles: 0, 1, 2, and 3, respectively. At an aging temperature of 500 °C, the mechanical strength of the 1P and 2P samples increased significantly, as shown in Figure 10a,c. For instance, the yield strength of the 1P and 2P samples increased from 291 MPa and 410 MPa to 558 MPa and 560 MPa, respectively. In comparison with the 1P and 2P samples, the increment in the 3P and 4P samples was not significant (<35 MPa). A similar phenomenon is observed regarding electrical conductivity. The IACS values for the 1P and 2P samples increased by 17.6% and 12.6%, respectively, while those for the 3P and 4P samples increased by 7.1% and 7.6%, respectively, as shown in Figure 10b. Interestingly, the elongation at break increased after aging for the samples from 1P to 3P, as depicted in Figure 10d. The elongation at break of the 2P sample increased from 11.1% to 16.5%, representing an increase of approximately 13.4%, and the tensile strength also increased by 28.8%. Furthermore, as the number of repeated extrusion cycles increased, the yield strength and tensile strength of the alloy exhibited a similar trend, initially increasing and then decreasing, with the maximum value attained at two extrusion cycles. However, the conductivity increased with the increasing number of extrusion cycles.

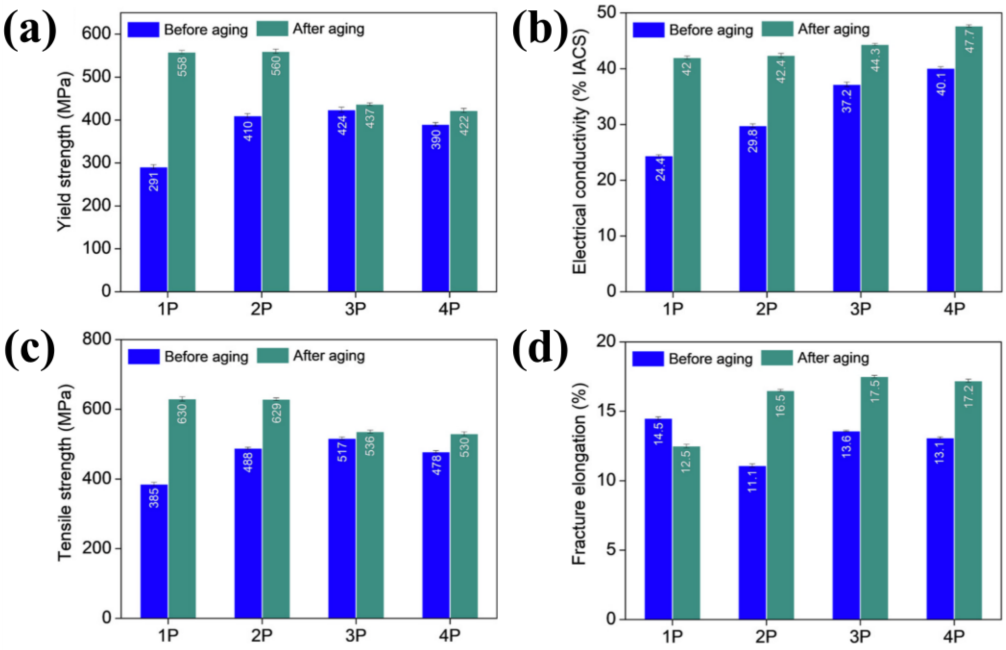

**Figure 10.** (**a**–**d**) Present the comparison of yield strength, electrical conductivity, tensile strength, and fracture elongation for 1P–4P samples before and after aging treatment at 500 °C, respectively [72].

In Cu-Ni-Si alloys, $Ni_2Si$ precipitates typically manifest in two forms: continuous precipitates (CPs) and discontinuous precipitates (DPs) [73,74]. Traditionally, CPs enhance the overall properties of alloys through the optimization of chemical composition and heat treatment. However, the tensile strength and conductivity of alloys containing only CPs are limited to 600–800 MPa and 40%–45% IACS, respectively, and do not fulfill the requirements of future high-end circuits [75–77]. Recent studies [54,78–81] have demonstrated that alloys containing DPs exhibit superior mechanical and electrical properties compared to those containing only CPs. By employing appropriate aging heat treatment, the distribution of DPs and CPs can be optimized to fully exploit the alloy's performance potential. L. Jiang et al. [82] reported that under identical deformation conditions, two-stage aging substantially enhanced the alloy's properties. Two-stage aging can dissolve some precipitates formed during the single-stage aging process back into the copper matrix, thereby introducing additional defects and strains. This process facilitates the formation of smaller, evenly dispersed precipitates. The results indicate that the tensile strength and conductivity of Cu-Ni-Si alloy treated with two-stage aging surpass those of alloys treated with single-stage aging. However, due to the numerous parameters involved in the multi-stage aging process, the related research is challenging and limited, leaving a significant gap in determining optimal process parameters.

With the growing use of machine learning models, Y. Shan [83] et al. used this technology to solve the above problems. They developed a machine learning model based on orthogonal tests to investigate the relationship between the two-stage aging parameters and the properties of the Cu-5.3Ni-1.3Si-0.12Nb alloy. The two-stage aging parameters of 400 °C/75 min + 400 °C/30 min, a tensile strength of 875 MPa, and an electrical conductivity of 41.43% IACS were achieved through multi-objective optimization combined with an experimental iteration strategy. The alloy's superior overall performance is primarily attributed to the co-precipitation of DPs and CPs, with a total integral number of 5.4% and a volume ratio of CPs to DPs of 6.7. This study offers a novel approach and insights for enhancing the comprehensive properties of Cu-Ni-Si alloys.

Aging treatment can improve the strength and conductivity of Cu-Ni-Si alloys. Based on current research findings, the aging temperature and time can be optimized to achieve the desired properties of the alloy by precisely adjusting the alloy composition and heat treatment parameters. In industrial production, given that workpieces are typically larger than experimental samples, a single aging treatment often cannot meet all performance requirements. Therefore, multi-stage heat treatment procedures, combined with various heat treatment technologies and stringent process control, are often employed to ensure that the finished product meets the specific needs of practical applications. This method helps to achieve consistency and reliability of alloy properties, meeting the needs of large-scale production.

## 7. Conclusions

Cu-Ni-Si alloys are regarded as promising for lead frame materials due to their excellent mechanical properties and adequate electrical conductivity. This paper provides an overview of the research progress on Cu-Ni-Si alloys as lead frame materials. The key points of the article are summarized as follows:

1. Cu-Ni-Si alloys have been widely studied for their excellent mechanical properties and electrical conductivity. Their strengthening mechanisms include solution strengthening, precipitation strengthening, and deformation strengthening. By controlling the atomic ratio of Ni to Si between 4 and 5, the overall properties of the alloy are significantly improved.
2. The alloy's properties are significantly affected by the preparation methods and processing technologies, including solution treatment, thermal deformation, and aging treatment. Solution treatment facilitates the formation of a saturated solid solution, which is crucial for subsequent aging. Hot deformation processes, such as hot rolling, can induce recrystallization and enhance mechanical properties, but may also introduce lattice distortions that diminish conductivity. Aging treatment is vital for precipitation strengthening, and precise control of aging parameters is essential to achieve the optimal balance of strength and conductivity.
3. The incorporation of trace and rare earth elements can enhance the alloy's performance. By precisely controlling the concentrations of these elements, the strength and conductivity of the alloy can be optimized to meet the requirements of various engineering and industrial applications.

In summary, while Cu-Ni-Si alloys possess extensive potential for research and application, further improvements in material properties, manufacturing processes, and sustainable development are necessary for their continued advancement.

## 8. Existing Problems and Future Prospects

In order to remain abreast of the swift advancements in science and technology, the development of advanced copper alloys and their components is crucial. Innovations in new materials, along with efficient preparation and processing technologies, can serve humanity more effectively and facilitate deeper exploration of new frontiers. These technological advancements not only promote scientific progress, but also provide humanity with new tools and methods to address complex challenges. Therefore, future research directions may focus on the following areas:

- To enhance the strength of copper alloys while maintaining their excellent conductivity, the development of novel preparation technologies is crucial. This entails investigating innovative processes, such as rapid solidification, to increase the solid solubility of the alloy. By employing such techniques, the mechanical properties of the alloy can be optimized without compromising electrical conductivity, resulting in a tensile strength ranging from 750 to 840 MPa and electrical conductivities of 35% IACS, which can meet the practical needs in integrated circuits.
- It is imperative to construct a comprehensive, systematic database that encompasses copper alloy material design, processing technology, and equipment application. Furthermore, the development of new copper alloys and their processing technologies, aligned with China's independent intellectual property rights, is essential.
- By incorporating alloying elements and adjusting alloy composition, in accordance with the principles of sustainable development, the goal should be to pursue industrialization and large-scale, systematic, green manufacturing. This would facilitate the production of high-precision, high-quality plate products with excellent stamping and etching abilities, weldability, and good plastic sealing performance.

In conclusion, Cu-Ni-Si alloy lead frames still need to be further improved and promoted in terms of material properties, manufacturing processes, application fields, and sustainable development. With ongoing technological innovation and industrial upgrading, Cu-Ni-Si alloy lead frames will play a key role in a broader range of applications in the future.

**Author Contributions:** All authors contributed to the study conception and design. Material preparation, data collection, and analysis were performed by H.Y., H.H., L.L., W.H. and C.L. The first draft of the manuscript was written by H.Y. and all authors commented on previous versions of the manuscript. All authors have read and agreed to the published version of the manuscript.

**Funding:** This work was supported by Grant No. 21ZR1424600 and No. 23010500800. Author HongLei Hu has received research support from the Natural Science Foundation of Shanghai and Three-year Action Plan of Shanghai Science and Technology Commission.

**Conflicts of Interest:** The authors declare no conflicts of interest.

## References

1. Chen, J.; Zhang, Z.; Wu, F. A data-driven method for enhancing the image-based automatic inspection of IC wire bonding defects. *Int. J. Prod. Res.* **2021**, *59*, 4779–4793. [CrossRef]
2. Han, D. Research status and key technology analysis of integrated circuit lead frame. *Acad. J. Eng. Technol. Sci.* **2023**, *6*, 43–49. [CrossRef]
3. Salvi, S.S.; Jain, A. A review of recent research on heat transfer in three-dimensional integrated circuits (3-D ICs). *IEEE Trans. Compon. Packag. Manuf. Technol.* **2021**, *11*, 802–821. [CrossRef]
4. Li, Y.; Wong, C. Recent advances of conductive adhesives as a lead-free alternative in electronic packaging: Materials, processing, reliability and applications. *Mater. Sci. Eng. R Rep.* **2006**, *51*, 1–35. [CrossRef]
5. Vianco, P.T. A Review of interface microstructures in electronic packaging applications: Brazing and welding technologies. *JOM* **2022**, *74*, 3557–3577. [CrossRef]
6. Wang, G.; Liu, H.; Song, K.; Zhou, Y.; Cheng, C.; Guo, H.; Guo, Y.; Tian, J. Aging process and strengthening mechanism of Cu–Cr–Ni alloy with superior stress relaxation resistance. *J. Mater. Res. Technol.* **2022**, *19*, 3579–3591. [CrossRef]
7. Ding, C.; Xu, J.; Shan, D.; Guo, B.; Langdon, T.G. Sustainable fabrication of Cu/Nb composites with continuous laminated structure to achieve ultrahigh strength and excellent electrical conductivity. *Compos. Part B Eng.* **2021**, *211*, 108662. [CrossRef]

8. Mao, Q.; Liu, Y.; Zhao, Y. A review on copper alloys with high strength and high electrical conductivity. *J. Alloys Compd.* **2024**, *990*, 174456. [CrossRef]
9. Yang, H.; Ma, Z.; Lei, C.; Meng, L.; Fang, Y.; Liu, J.; Wang, H. High strength and high conductivity Cu alloys: A review. *Sci. China Technol. Sci.* **2020**, *63*, 2505–2517. [CrossRef]
10. Jiang, Y.; Lou, H.; Xie, H.; Li, T.; Song, K.; Liu, X.; Yun, X.; Wang, H.; Xiao, Z.; Li, Z. Development status and prospects of advanced copper alloy. *Strateg. Study Chin. Acad. Eng.* **2020**, *22*, 84–92. [CrossRef]
11. Wu, A.-Q.; Wang, S.-W.; Chen, S.-F.; Li, Y.; Liu, J.-S.; Chen, Y.; Song, H.-W. Research status and development trend of copper-nickel-silicon alloy for lead frame. *Copp. Eng.* **2021**, *4*, 14–20. [CrossRef]
12. Mi, X.; Lou, H.; Xie, H.; Mo, Y.; Zhang, W.; Xiang, C. Development strategy for advanced copper-based materials in China. *Strateg. Study Chin. Acad. Eng.* **2023**, *25*, 96–103. [CrossRef]
13. Ge, S.; Isac, M.; Guthrie, R.I.L. Progress in strip casting technologies for steel; technical developments. *ISIJ Int.* **2013**, *53*, 729–742. [CrossRef]
14. Fan, L.; Liu, P.; Jia, S.; Tian, B.; Zhang, Y. Research progress of copper based lead frame materials. *Mater. Dev. Appl.* **2008**, *23*, 101–107. [CrossRef]
15. Liao, W.; Zhang, C.; Qiang, H.; Song, W.; Ren, H. Effect and Mechanism of Solidified Microstructure on Deformation Behavior, Mechanical Properties, and Residual Stress of Cu-Ni-Si Alloy. *Materials* **2022**, *15*, 8724. [CrossRef] [PubMed]
16. Xiang, K.; Lei, X.; Ding, L.; Jia, Z.; Yang, X.; Liu, Q. Optimizing mechanical property of spray formed Al-Zn-Mg-Cu alloy by combination of homogenization and warm-rolling. *Mater. Sci. Eng. A* **2022**, *846*, 143248. [CrossRef]
17. Yang, G.; Xu, W.; Jin, X.; Wang, Z.; Shan, D.; Guo, B. Hot deformation behavior and microstructure evolution of the spray deposited and secondary hot extruded 2195 Al–Li alloy. *J. Mater. Res. Technol.* **2022**, *20*, 2784–2798. [CrossRef]
18. Agrawal, A.; Vajpai, S.K. Preparation of Cu–Al–Ni shape memory alloy strips by spray deposition-hot rolling route. *Mater. Sci. Technol.* **2020**, *36*, 1337–1348. [CrossRef]
19. Sato, S.; Maki, K.; Ito, M.; Suzuki, S. Factors Affecting the Physical Properties of Electrically Conductive Copper and Dilute Copper Alloys. *Mater. Trans.* **2023**, *64*, 2039–2050. [CrossRef]
20. Wang, W.; Chen, Z.; Guo, E.; Zhang, S.; Kang, H.; Wang, T. Effects of Cr Addition on the Precipitation and Properties of Cryo-Rolled CuNiSi Alloys. *Metals* **2023**, *13*, 758. [CrossRef]
21. Wu, Y.; Li, Y.; Lu, J.; Tan, S.; Jiang, F.; Sun, J. Correlations between microstructures and properties of Cu-Ni-Si-Cr alloy. *Mater. Sci. Eng. A* **2018**, *731*, 403–412. [CrossRef]
22. Guo, M.; Shen, K.; Wang, M. Relationship between microstructure, properties and reaction conditions for Cu–$TiB_2$ alloys prepared by in situ reaction. *Acta Mater.* **2009**, *57*, 4568–4579. [CrossRef]
23. Lei, Q.; Xiao, Z.; Hu, W.; Derby, B.; Li, Z. Phase transformation behaviors and properties of a high strength Cu-Ni-Si alloy. *Mater. Sci. Eng. A* **2017**, *697*, 37–47. [CrossRef]
24. Han, S.Z.; Kang, J.; Kim, S.-D.; Choi, S.-Y.; Kim, H.G.; Lee, J.; Kim, K.; Lim, S.H.; Han, B. Reliable and cost effective design of intermetallic $Ni_2Si$ nanowires and direct characterization of its mechanical properties. *Sci. Rep.* **2015**, *5*, 15050. [CrossRef]
25. Hu, T.; Chen, J.; Liu, J.; Liu, Z.; Wu, C. The crystallographic and morphological evolution of the strengthening precipitates in Cu–Ni–Si alloys. *Acta Mater.* **2013**, *61*, 1210–1219. [CrossRef]
26. Monzen, R.; Watanabe, C. Microstructure and mechanical properties of Cu–Ni–Si alloys. *Mater. Sci. Eng. A* **2008**, *483*, 117–119. [CrossRef]
27. Suzuki, S.; Shibutani, N.; Mimura, K.; Isshiki, M.; Waseda, Y. Improvement in strength and electrical conductivity of Cu–Ni–Si alloys by aging and cold rolling. *J. Alloys Compd.* **2006**, *417*, 116–120. [CrossRef]
28. Zhao, D.; Dong, Q.; Liu, P.; Kang, B.; Huang, J.; Jin, Z. Structure and strength of the age hardened Cu–Ni–Si alloy. *Mater. Chem. Phys.* **2003**, *79*, 81–86. [CrossRef]
29. Teplitskii, M.; Nikolaev, A.; Revina, N.; Rozenberg, V. Investigation of the Dispersed Particles in Ageing Alloys of Cu-Ni-Si and Cu-Co-Si. *Phys. Met. Metallogr.* **1975**, *40*, 99–103.
30. Lei, Q.; Li, Z.; Zhu, A.; Qiu, W.; Liang, S. The transformation behavior of Cu–8.0Ni–1.8Si–0.6Sn–0.15Mg alloy during isothermal heat treatment. *Mater. Charact.* **2011**, *62*, 904–911. [CrossRef]
31. Yi, J.; Jia, Y.; Zhao, Y.; Xiao, Z.; He, K.; Wang, Q.; Wang, M.; Li, Z. Precipitation behavior of Cu-3.0Ni-0.72Si alloy. *Acta Mater.* **2019**, *166*, 261–270. [CrossRef]
32. Lutfi, M.; Binti Yusof, F.; Ariga, T.; Singh, R.; Bin Abd Shukor, M.H. Interfacial reaction analysis of Cu-Sn-Ni-P/Cu joint using microwave hybrid heating. *Key Eng. Mater.* **2016**, *701*, 148–153. [CrossRef]
33. Thi Chieu, L.; Thang, S.M.; Nam, N.D.; Pham, M.K. The effect of deformation on microstructure of Cu-Ni-Sn aging alloys. *Key Eng. Mater.* **2016**, *682*, 113–118. [CrossRef]
34. Goto, M.; Utsunomiya, T.; Yamamoto, T.; Han, S.Z.; Kitamura, J.; Ahn, J.-H.; Lim, S.H.; Yakushiji, T. Microstructure and fatigue properties of Cu–Ni–Si alloy strengthened by $Ni_2Si$ intermetallic compounds. *Comput. Methods Exp. Meas. XX* **2021**, *130*, 75. [CrossRef]

35. Hu, J.; Jiang, Y.; Zhao, F.; Liu, X.; Li, Z.; Lu, C.; Liu, A. Microstructure, properties and deformation mechanism of HCCM horizontal continuous casting Cu–Ni–Co–Si alloy strip during cold rolling. *J. Mater. Res. Technol.* **2023**, *23*, 5474–5485. [CrossRef]
36. Xu, Z.; Shi, H.; Liu, S.; Li, X.; Gan, W.; Hu, X.; Fan, G.; Wang, X. Effect of aging temperature on microstructure and properties of cold-rolled Cu-Ni-Si alloy. *Mater. Today Commun.* **2024**, *40*, 109438. [CrossRef]
37. Taylor, G.I. The use of flat-ended projectiles for determining dynamic yield stress I. Theoretical considerations. *Proc. R. Soc. Lond. Ser. A Math. Phys. Sci.* **1948**, *194*, 289–299. [CrossRef]
38. Wei, H.; Chen, Y.-L.; Su, L.; Tang, D.; Xu, Z.-J. Study on texture evolution and deformation mechanism of the Cu-Ni-Si alloy during cold-rolling treatment. *Procedia Eng.* **2017**, *207*, 1111–1116. [CrossRef]
39. Liu, F.; Mi, X.; Ma, J. Microstructure and properties of low concentration Cu-Ni-Si alloys. *Chin. J. Nonferr. Met.* **2019**, *29*, 286–294. [CrossRef]
40. Zhu, X.; Chen, H.; Zhang, Z.; Yan, B.; Wu, G. Microstructure evolution and composite strengthening mechanism during solid solution and aging treatment for Cu-Ni-Co-Si sheet. *Mater. Today Commun.* **2024**, *40*, 109707. [CrossRef]
41. Courtney, T.H. *Mechanical Behavior of Materials*; Waveland Press: Long Grove, IL, USA, 2005.
42. Batra, I.; Dey, G.; Kulkarni, U.; Banerjee, S. Microstructure and properties of a Cu–Cr–Zr alloy. *J. Nucl. Mater.* **2001**, *299*, 91–100. [CrossRef]
43. Ren, W.; Jia, S.-G.; Liu, P.; Song, K.-X. Effect of solution temperature on properties of Cu-Ni-Si alloy. *Hot Work. Technol.* **2009**, *38*, 121–123. [CrossRef]
44. Lockyer, S.; Noble, F. Precipitate structure in a Cu-Ni-Si alloy. *J. Mater. Sci.* **1994**, *29*, 218–226. [CrossRef]
45. Li, J.; Huang, G.; Mi, X.; Peng, L.; Xie, H.; Kang, Y. Effect of Ni/Si mass ratio and thermomechanical treatment on the microstructure and properties of Cu-Ni-Si alloys. *Materials* **2019**, *12*, 2076. [CrossRef] [PubMed]
46. Tao, S.; Lu, Z.; Jia, L.; Xie, H.; Zhang, J. Effect of Ni/Si mass ratio on microstructure and properties of Cu–Ni–Si alloy. *Mater. Res. Express* **2020**, *7*, 066520. [CrossRef]
47. Jia, Y.-L.; Wang, M.-P.; Chen, C.; Dong, Q.-Y.; Wang, S.; Li, Z. Orientation and diffraction patterns of δ-$Ni_2Si$ precipitates in Cu–Ni–Si alloy. *J. Alloys Compd.* **2013**, *557*, 147–151. [CrossRef]
48. Liu, J.; Cao, Y.-C.; Mi, X.-J.; Xie, H.-F.; Mi, Z.-L.; Peng, L.-J. Research status and development Trend of high Performance Cu-Ni-Si Alloy. *Copp. Eng.* **2024**, *3*, 152–162. [CrossRef]
49. Han, S.Z.; Jeong, I.-S.; Ryu, B.; Lee, S.J.; Ahn, J.H.; Choi, E.-A. Enhanced strength of Cu-Ni-Si alloy via heterogeneous nucleation at grain boundaries during homogenization. *Mater. Charact.* **2024**, *215*, 114198. [CrossRef]
50. Liu, J.; Wang, X.; Chen, J.; Liu, J. The effect of cold rolling on age hardening of Cu-3Ti-3Ni-0.5Si alloy. *J. Alloys Compd.* **2019**, *797*, 370–379. [CrossRef]
51. Zhao, Z.; Zhang, Y.; Tian, B.; Jia, Y.; Liu, Y.; Song, K.; Volinsky, A.A. Co effects on Cu-Ni-Si alloys microstructure and physical properties. *J. Alloys Compd.* **2019**, *797*, 1327–1337. [CrossRef]
52. Krupińska, B.; Borek, W.; Krupiński, M.; Karkoszka, T. The influence of Ag on the microstructure and properties of Cu-Ni-Si alloys. *Materials* **2020**, *13*, 3416. [CrossRef]
53. Huang, F.; Ma, J.; Ning, H.; Cao, Y.; Geng, Z. Precipitation in Cu–Ni–Si–Zn alloy for lead frame. *Mater. Lett.* **2003**, *57*, 2135–2139. [CrossRef]
54. Meng, X.; Xie, G.; Xue, W.; Fu, Y.; Wang, R.; Liu, X. The precipitation behavior of a Cu-Ni-Si alloy with Cr addition prepared by heating-cooling combined mold (HCCM) continuous casting. *Materials* **2022**, *15*, 4521. [CrossRef] [PubMed]
55. Wang, W.; Kang, H.; Chen, Z.; Chen, Z.; Zou, C.; Li, R.; Yin, G.; Wang, T. Effects of Cr and Zr additions on microstructure and properties of Cu-Ni-Si alloys. *Mater. Sci. Eng. A* **2016**, *673*, 378–390. [CrossRef]
56. Lei, Q.; Li, Z.; Dai, C.; Wang, J.; Chen, X.; Xie, J.; Yang, W.; Chen, D. Effect of aluminum on microstructure and property of Cu–Ni–Si alloys. *Mater. Sci. Eng. A* **2013**, *572*, 65–74. [CrossRef]
57. Wang, W.; Wang, J.; Li, S.; Wang, C.; Zhou, J.; Zeng, J.; Tan, W.; Wang, B. Effects of Nb addition on the properties and microstructure of Cu-Ni-Si-Mg alloy. *Mater. Charact.* **2022**, *194*, 112451. [CrossRef]
58. Wan, J.; Xiao, X.-P.; Xiong, S.-J.; Chen, J.-S.; Guo, C.-J. Effect of Si additions on mechanical properties and softening resistance of Cu–Ni-Sn-P alloy. *Mater. Today Commun.* **2023**, *34*, 105394. [CrossRef]
59. Liu, Q.; Wang, T.; Jiao, J.; Wang, W.; Liu, H.; Zhang, X.; Zhang, C.; Qi, F.; Jie, J.; Xu, X. The microstructures and properties of diamond reinforced Cu–Ni–Si–Ti alloys. *Mater. Sci. Eng. A* **2023**, *862*, 144478. [CrossRef]
60. Tan, L.; Li, Y.; Ng, S.; Lu, L. Effects of rare earth additions on structures and properties of rapidly solidified copper alloys. *Mater. Sci. Technol.* **1999**, *15*, 169–179. [CrossRef]
61. Rdzawski, Z.; Głuchowski, W.; Stobrawa, J.; Sobota, J. Effect of rare-earth metals addition on microstructure and properties of selected copper alloys. *Arch. Metall. Mater.* **2014**, *59*, 641–648. [CrossRef]
62. Liu, J.-S.; Wu, A.-S.; Wang, S.-W.; Chen, S.-F.; Zhang, M.-X.; Song, H.-W.; Zhang, S.-H. Effect of lanthanum on microstructure and properties of Cu-Ni-Si alloy as cast. *Chin. J. Rare Earth Sci.* **2023**, *41*, 930–941.

63. Wang, X.-J.; Xie, C.-X.; Liu, R.-Q. The influence of Ce on Cu–Ni–Si alloy microstructure and performance. *Shanghai Non-Ferr. Met.* **2009**, *30*, 150–152. [CrossRef]
64. Wang, T.-Y. Effect of trace Er and Gd on microstructure and properties of Cu-Ni-Si alloys. *Nonferr. Met. Des.* **2022**, *49*, 55–59. [CrossRef]
65. Wang, H.-S.; Chen, H.-G.; Gu, J.-W.; Hsu, C.-E.; Wu, C.-Y. Effects of heat treatment processes on the microstructures and properties of powder metallurgy produced Cu–Ni–Si–Cr alloy. *Mater. Sci. Eng. A* **2014**, *619*, 221–227. [CrossRef]
66. Li, H.; Wang, X.; Song, Y.; Li, Y.; Li, X.; Ji, Y. Physical metallurgy guided machine learning to predict hot deformation mechanism of stainless steel. *Mater. Today Commun.* **2023**, *36*, 106779. [CrossRef]
67. Cao, G.; Wang, Z.; Li, C.; Jia, F.; Zhang, Y. Evolution of structure and property for Cu–Ni–Si alloy based on hot-rolling process. *Chin. J. Nonferr. Met.* **2018**, *28*, 2024–2032. [CrossRef]
68. Wang, Y.; Zhang, L.; Guo, B.; Li, K.; Ni, S.; Du, Y.; Song, M. Effects of hot rolling, intermediate annealing and cold rolling on microstructure, texture and mechanical properties of an Al-Mg-Si-Cu alloy. *Mater. Res. Express* **2018**, *5*, 106521. [CrossRef]
69. Jia, Y.; Pang, Y.; Yi, J.; Lei, Q.; Li, Z.; Xiao, Z. Effects of pre-aging on microstructure and properties of Cu-Ni-Si alloys. *J. Alloys Compd.* **2023**, *942*, 169033. [CrossRef]
70. Li, Y.-H.; Chen, S.-F.; Wang, S.-W.; Song, H.-W.; Zhang, S.-H. Coarsening mechanism of over-aged δ-$Ni_2Si$ nanoscale precipitates in Cu-Ni-Si-Cr-Mg alloy. *Mater. Charact.* **2024**, *209*, 113693. [CrossRef]
71. Lee, S.J.; Shin, H.S.; Choi, E.; Ahn, J.H.; Choi, Y.; Kim, S.; Lee, J.; Han, S.Z. Effect of Pre-Aging Treatment on the Mechanical Properties of Cold Rolled Cu-6 wt% Ni-1.4 wt% Si Alloy. *Korean J. Met. Mater.* **2020**, *58*, 488–494. [CrossRef]
72. Qi, F.; Fu, H.; Yin, Y.; Yun, X. Improved mechanical strength, ductility, and electrical conductivity of Cu–Ni–Si alloys after multi-pass continuous extrusion and aging processes. *Mater. Charact.* **2024**, *208*, 113681. [CrossRef]
73. Semboshi, S.; Sato, S.; Iwase, A.; Takasugi, T. Discontinuous precipitates in age-hardening CuNiSi alloys. *Mater. Charact.* **2016**, *115*, 39–45. [CrossRef]
74. Goto, M.; Yamamoto, T.; Han, S.; Utsunomiya, T.; Kim, S.; Kitamura, J.; Ahn, J.; Lim, S.; Lee, J. Simultaneous increase in electrical conductivity and fatigue strength of Cu-Ni-Si alloy by utilizing discontinuous precipitates. *Mater. Lett.* **2021**, *288*, 129353. [CrossRef]
75. Ban, Y.; Geng, Y.; Hou, J.; Zhang, Y.; Zhou, M.; Jia, Y.; Tian, B.; Liu, Y.; Li, X.; Volinsky, A.A. Properties and precipitates of the high strength and electrical conductivity Cu-Ni-Co-Si-Cr alloy. *J. Mater. Sci. Technol.* **2021**, *93*, 1–6. [CrossRef]
76. Yang, K.; Wang, Y.; Guo, M.; Wang, H.; Mo, Y.; Dong, X.; Lou, H. Recent development of advanced precipitation-strengthened Cu alloys with high strength and conductivity: A review. *Prog. Mater. Sci.* **2023**, *138*, 101141. [CrossRef]
77. Liao, W.; Yang, H.; Yi, C.; Zheng, J. Effect and mechanism of cold rolling and aging process on microstructure and properties of columnar grain C70250 copper alloy. *Mater. Sci. Eng. A* **2022**, *833*, 142577. [CrossRef]
78. Ahn, J.H.; Han, S.Z.; Choi, E.-A.; Lee, H.; Lim, S.H.; Lee, J.; Kim, K.; Hwang, N.M.; Han, H.N. The effect of bimodal structure with nanofibers and normal precipitates on the mechanical and electrical properties of CuNiSi alloy. *Mater. Charact.* **2020**, *170*, 110642. [CrossRef]
79. Kim, H.; Ahn, J.H.; Han, S.Z.; Jo, J.; Baik, H.; Kim, M.; Han, H.N. Microstructural characterization of cold-drawn Cu–Ni–Si alloy having high strength and high conductivity. *J. Alloys Compd.* **2020**, *832*, 155059. [CrossRef]
80. Ahn, J.H.; Han, S.Z.; Choi, E.-A.; Lee, G.Y.; Kim, K.; Lee, J.; Han, H.N. Simple optimization for strength and conductivity of Cu-Ni-Si alloy with discontinuous precipitation. *Mater. Charact.* **2022**, *184*, 111605. [CrossRef]
81. Cao, Y.; Han, S.Z.; Choi, E.-A.; Ahn, J.H.; Mi, X.; Huang, G.; Lee, S.; Shin, H.; Kim, S.; Lee, J. Effect of pre-deformation before aging on discontinuous precipitation behaviour in Cu-Ni-Si alloys. *Philos. Mag. Lett.* **2021**, *101*, 51–59. [CrossRef]
82. Jiang, L.; Fu, H.; Wang, C.; Li, W.; Xie, J. Enhanced mechanical and electrical properties of a Cu-Ni-Si alloy by thermo-mechanical processing. *Metall. Mater. Trans. A* **2020**, *51*, 331–341. [CrossRef]
83. Shan, Y.; Zhang, Y.; Zhang, C.; Feng, J.; Huang, B.; Zhao, S.; Song, K. Study on the microstructure and mechanism of stress relaxation behavior of Cu–Ni–Si alloy by two-stage rolling deformation. *Mater. Sci. Eng. A* **2024**, *908*, 146946. [CrossRef]